

Learning Registered Point Processes from Idiosyncratic Observations

Hongteng Xu¹

¹Department of Electrical and Computer Engineering, Duke University

²College of Computing, Georgia Institute of Technology

Lawrence Carin¹

Hongyuan Zha²

Abstract

A parametric point process model is developed, with modeling based on the assumption that sequential observations often share latent phenomena, while also possessing idiosyncratic effects. An alternating optimization method is proposed to learn a “registered” point process that accounts for shared structure, as well as “warping” functions that characterize idiosyncratic aspects of each observed sequence. Under reasonable constraints, in each iteration we update the sample-specific warping functions by solving a set of constrained nonlinear programming problems in parallel, and update the model by maximum likelihood estimation. The justifiability, complexity and robustness of the proposed method are investigated in detail. Experiments on both synthetic and real-world data demonstrate that the method yields explainable point process models, achieving encouraging results compared to state-of-the-art methods.

1 Introduction

The behavior of real-world entities often may be recorded as event sequences; for example, interactions of participants in a social network, the admissions of patients, and the job-hopping behavior of employees. In practice, these behaviors are under the control of complicated mechanisms, which can be captured approximately by an appropriate parametric temporal point process model. While the observed event sequences associated with a given process (*e.g.*, disease) may share common (“standard”) attributes, there are often subject-specific factors that may impact the observed data. For example, the admission records of different patients are always personalized: even if the patients

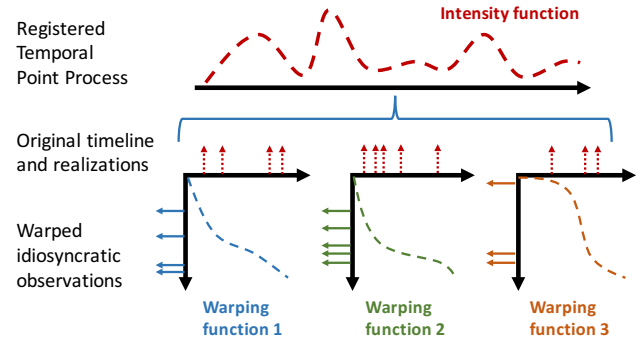


Figure 1: The illustration of concepts in our work. The dotted parts (parametric point process model, unwarped realizations and warping functions) are what we aim to learn.

suffer from the same disease, they may spend unequal time on recovery because their medications, history and environmental conditions may be distinct. Another typical example is the job-hopping behavior of employees. The employees in the same company often make very different career plans depending on the status of the job market, their age, family situation and salaries. Even if two individuals have the same preferred company, they are likely to change jobs at different times, due to detailed aspects of their situations, with these often unobserved.

The examples above reveal that event sequences that share an underlying temporal point process linked to a given phenomenon of interest may be personalized by hidden idiosyncratic factors, yielding a subject-specific “warping” along timeline, as shown in Fig. 1. The characteristics of such data often have a negative influence on the learning of the target point process, *i.e.*, increase the uncertainty of the model and the risk of model misspecification. The complexity of models can be increased to fit the personalized observations well, *e.g.*, the locally-stationary point processes in [25, 18, 34]. However, from the viewpoint of model registration, it is desirable to separate the essential mechanism of the model and idiosyncratic aspects of the data, such that the final model is “registered” and characterizes the shared phenomena associated with a given class of data, while also inferring what is sample-specific.

Learning registered point processes from idiosyncratic observations is a challenging problem, requiring one to jointly

learn a shared point process model and a set of sample-specific warping functions corresponding to observed event sequences. To solve this problem, we propose a novel and effective learning method in an iterative framework of alternating optimization. Specifically, in each iteration we first apply the inverse of estimated warping functions (*i.e.*, unwarping functions) to unwarped observed event sequences and learn the parameter of a registered point process by maximizing the likelihood of the unwarped event sequences; we then update the warping functions of event sequences, based on the estimation of registered point process. The new functions are applied to update the model for the next iteration. In particular, we approximate the warping/unwarping functions of event sequences by piecewise linear models, and learn their parameters by solving a set of constrained nonlinear programming problems in parallel. Such an alternating optimization method is suitable for a large class of parametric point process models, *e.g.*, Hawkes processes [10] and self-correcting processes [12, 36].

We analyze the justification and the complexity of our learning method in detail. The meaning of the regularizers and constraints used in our method and their influence on learning results are also investigated. Experimental results show that the proposed method outperforms its competitors on both synthetic and real-world data.

2 Related Work

2.1 Temporal point processes

Denote a temporal point process as N . Its realization (*i.e.*, an event sequence) consists of multiple events $\{(t_i, c_i)\}_{i=1}^M$ with time stamps $t_i \in [0, T]$ and event types $c_i \in \mathcal{C} = \{1, \dots, C\}$, which can be equivalently represented as $\{N_c(t)\}_{c=1}^C$, where $N_c(t)$ is the number of type- c events occurring at or before time t . A temporal point process can be characterized by its intensity functions $\{\lambda_c(t)\}_{c=1}^C$, where $\lambda_c(t) = \mathbb{E}[dN_c(t)|\mathcal{H}_t^C]/dt$ and $\mathcal{H}_t^C = \{(t_i, c_i) | t_i < t, c_i \in \mathcal{C}\}$ collects historical events before time t . Each $\lambda_c(t)$ represents the expected instantaneous rate of the type- c event at time t , conditioned on the history.

Parametric point processes may be categorized via the formulations of their intensity functions. For example, the Hawkes process [10] has an additive intensity:

$$\lambda_c(t) = \mu_c + \sum_{c'=1}^C \int_0^t \phi_{cc'}(s) dN_{c'}(t-s), \quad (1)$$

where μ_c is the background intensity independent of the history, while $\sum_{c'=1}^C \int_0^t \phi_{cc'}(s) dN_{c'}(t-s)$ is the endogenous intensity capturing the triggering patterns between events. The impact function $\phi_{cc'}(t)$ captures the decay in the influence of historical type- c' events on the subsequent type- c events. When it is an exponential function [40] or

a sum of exponential functions, the intensity function of Hawkes process is an exponential-like additive model; Differing from the Hawkes process, the self-correcting process [12, 36] has an multiplicative intensity function:

$$\lambda_c(t) = \exp(\mu_c(t - t_0) - \sum_{t_i < t} \phi_{cc_i}(t_i)), \quad (2)$$

which can be represented as the product of multiple exponential functions of time. Here t_0 is a referred starting time.

Point processes have been proven to be useful in many applications, *e.g.*, financial analysis [3], social network analysis [40, 39], health record analysis [35, 34], and computer vision [36]. However, most existing work does not consider learning parametric point processes from idiosyncratic (or warped) observations with latent sample-specific effects. The methods in [15, 37] try to estimate time scaling parameters for their point process models, but they are only available for Hawkes processes whose event sequences share the same linear transformation of time, which cannot capture personalized and nonlinear phenomena. The work in [17] is able to jointly learn specific point processes for different event sequences by multi-task learning, but it does not register its learning results or learn sample-specific warping functions explicitly.

2.2 Data registration and model registration

As aforementioned, the idiosyncratic aspects of sequential data may be viewed in terms of a sample-specific “warping” of a common latent phenomena. Traditional time warping (and unwarping) methods, *e.g.*, the dynamic time warping (DTW) [4, 19] and the curve registration method [24], aim to measure the difference between functional data or curves, by registering the data according to a learned or predefined transformation. Besides matching data robustly, for those non-parametric models like Gaussian processes, warping data is beneficial to improve the robustness of learning methods [27, 6, 28, 11]. From the viewpoint of methodology, many methods, including the DTW and its variants [31, 7], the self-modeling registration method (SMR) [9], the moment-based method (MBM) [13], the pairwise curve synchronization method (PACE) [30], and the functional convex averaging (FCA) method [16] can be categorized in the same framework – the registered curves and the corresponding warping functions are learned alternatively based on a nonlinear least-squares criterion. Instead of using the Euclidean metric, the recent work in [29] obtains better data registration results by using the Fisher-Rao metric (FRM). Unfortunately, all the methods above focus on warping/unwarping continuous curves in a nonparametric way, which cannot register parametric point processes from warped (idiosyncratic) asynchronous event sequences.

Beyond data registration, we need to develop advanced methods to register point processes from warped data. Fo-

cusing on this problem, the work in [22, 38] proposes a model-registration method. Specifically, the unregistered distributions of warped observations are first estimated by nonparametric models, and then the registered point process are estimated as the barycenter (or equivalently, the Fréchet mean) of the distributions in Wasserstein space [20]. Finally, the warping function between any unregistered distribution and the registered one is learned as an optimal transport [1]. This method is able to learn sample-specific warping functions explicitly, but is only suitable for simple nonparametric models like inhomogeneous Poisson processes with nonparametric intensity functions. The recent combination of Wasserstein learning and neural networks [2, 33] achieves encouraging improvements on learning robust generative models from imperfect (*i.e.*, sparse and noisy) observations. However, the neural network-based model requires many time-consuming simulation steps in the learning phase. Further, it cannot in general learn interpretable parametric models or explicit warping functions.

3 Proposed Learning Method

3.1 Problem statement and formulation

Given a set of event sequences generated by a shared parametric point process but warped in a hidden idiosyncratic manner, we seek to learn a “registered” model, as well as sample-specific warping functions. Specifically, assume i.i.d. event sequences of a parametric point process model N_θ are warped in $[0, T]$ by a set of continuous and invertible warping functions. Denote the sequences and the corresponding warping functions as $\{S_m\}_{m=1}^M$ and $\{W_m\}_{m=1}^M$, respectively. Each $S_m = \{(t_i^m, c_i^m)\}_{i=1}^{I_m}$ contains I_m events, whose time stamps are deformed from a “standard” timeline under the corresponding warping function $W_m : [0, T] \mapsto [0, T]$. Accordingly, the unwarping functions, *i.e.*, the inverse warping functions, can be denoted as $\{W_m^{-1}\}_{m=1}^M$. Following [30, 22], we assume that for $m = 1, \dots, M$

1 *Unbiasedness*: $\mathbb{E}[W_m(t)] = t$ on $[0, T]$.

2 *Regularity*: $W_m(t)$ is monotone increasing on $[0, T]$.

Note that these two assumptions are equivalently imposed on the unwarped functions as well. Additionally, we impose an assumption on the target point process:

3 *Exponential-like intensity*: the intensity function of the target point process at arbitrary time can be represented as a weighted sum of exponential functions of time, *i.e.*, $\lambda(t) = \sum_{j=1}^J \alpha_j \exp(-\beta_j t)$. The parameters α_j ’s and β_j ’s and their numbers J can be specified according to the history \mathcal{H}_t^C .

This assumption is helpful to simplify our learning algorithm, shown in the following. Because many important point process models, *e.g.*, the Hawkes process and the self-correcting process mentioned above satisfy this assumption, it does not affect the universality of our learning algorithm in practice. A detailed derivation is given in Appendix 6.1.

The warped data caused by idiosyncratic effects generally do harm to the learning of the target point process. Theoretically, we prove in Appendix 6.2 that

Theorem 3.1. *For a temporal point process N_θ satisfying the assumption 3, $\hat{\theta}^*$ and $\hat{\theta}$ denote its maximum likelihood estimation based on original data and that based on warped data, respectively. The warping functions satisfy the assumptions 1 and 2. Then $\hat{\theta}^* = \hat{\theta}$ if and only if 1) the warping functions are translations; or 2) N_θ is a homogeneous Poisson process.*

Therefore, we aim to estimate the parameter θ of the target point process and the warping functions $\{W_m\}_{m=1}^M$ (or equivalently, the unwarping functions $\{W_m^{-1}\}_{m=1}^M$) from the warped observations $\{S_m\}_{m=1}^M$. To achieve this, we develop a learning method based on maximum likelihood estimation (MLE). Instead of applying MLE directly to warped observations, we consider the influence of warping functions and maximize the likelihood of estimated unwarped sequences. The likelihood function of an unwarped sequence can be formulated based on the intensity function of the point process [8]:

$$\mathcal{L}(\theta; W_m^{-1}(S_m)) = \frac{\prod_{i=1}^{I_m} \lambda_{c_i^m}(W_m^{-1}(t_i^m))}{\exp\left(\sum_{c=1}^C \int_0^T \lambda_c(W_m^{-1}(s)) ds\right)}, \quad (3)$$

where $W_m^{-1}(S_m)$ represents the unwarped event sequence, *i.e.*, $W_m^{-1}(S_m) = \{(W_m^{-1}(t_i^m), c_i^m)\}_{i=1}^{I_m}$.

Considering the assumptions of warping functions and the definition of likelihood, we can formulate the optimization problem as

$$\begin{aligned} \min_{\theta, \{W_m\}} \quad & - \sum_m \log \mathcal{L}(\theta; W_m^{-1}(S_m)) + \gamma \mathcal{R}(\{W_m\}) \\ \text{s.t.} \quad & 1) \quad W_m(0) = 0, \quad W_m(T) = T, \quad \text{and} \\ & 2) \quad W_m'(t) > 0 \quad \text{for } m = 1, \dots, M, \end{aligned} \quad (4)$$

where $W_m'(t) = \frac{dW_m}{dt}$ is the derivative of warping function. In our objective function, the first term represents the negative log-likelihood of unwarped event sequences while the second term represents the regularizer imposed on warping/unwarping functions. For each warping function, the first constraint corresponds to its range and the second constraint makes it obey the regularity assumption. Furthermore, according to the unbiasedness assumption, we apply the following regularizer:

$$\mathcal{R}(\{W_m\}) = \int_0^T \left| \frac{1}{M} \sum_{m=1}^M W_m^{-1}(s) - s \right|^2 ds. \quad (5)$$

Here we regularize unwarping functions rather than warping functions to simplify the learning process, as shown in Section 3.3.

3.2 Maximizing the likelihood

The optimization problem in (4) is non-convex and has a large number of unknown variables. Solving it directly is intractable. Fortunately, for the parametric point processes with exponential-like intensity functions, we can design an effective alternating optimization method to solve the problem iteratively, after parameterizing the warping functions as piecewise linear functions. In each iteration, we first maximize the likelihood of the unwarped sequences based on the estimation of warping functions, and then optimize the warping functions based on the estimated model.

Specifically, in the k -th iteration, given the warping functions estimated in the previous iteration, *i.e.*, $\{W_m^{k-1}\}_{m=1}^M$, we learn the target point process by

$$\theta^k = \arg \min_{\theta} - \sum_{m=1}^M \log \mathcal{L}(\theta; (W_m^{k-1})^{-1}(S_m)). \quad (6)$$

Focusing on different point processes, we can apply various optimization methods to solve this problem. For example, learning Hawkes processes can be achieved in the framework of expectation-maximization (EM) [15, 40], which is equivalent to a projected-gradient-ascent algorithm. For other kinds of parametric point processes, *e.g.*, the self- and mutually-correcting processes, we can learn their parameters by gradient descent or stochastic gradient descent (SGD) [36, 35].

3.3 Learning warping/unwarping functions

Given θ^k , we need to update the warping/unwarping functions. To simplify the problem and accelerate our learning method, we take advantage of the warping functions estimated in the previous iteration, *i.e.*, $\{W_m^{k-1}\}_{m=1}^M$, and decompose the problem into M independent problems: for $m = 1, \dots, M$, W_m^k is the solution of

$$\begin{aligned} & \min_{W_m} - \log \mathcal{L}(\theta^k; W_m^{-1}(S_m)) \\ & + \gamma \int_0^T \left| \frac{W_m^{-1}(s)}{M} + \frac{\sum_{m' \neq m} (W_{m'}^{k-1})^{-1}(s)}{M} - s \right|^2 ds \quad (7) \\ & \text{s.t. } W_m(0) = 0, \quad W_m(T) = T, \quad W_m'(t) > 0. \end{aligned}$$

Solving these problems is non-trivial, requiring further parameterization of the warping functions $\{W_m\}_{m=1}^M$, or equivalently, the unwarping functions $\{W_m^{-1}\}_{m=1}^M$.

We apply a set of piecewise linear models to fit the unwarping functions, for the convenience of mathematical derivation and computation. Specifically, given L landmarks $\{t_1, \dots, t_L\}$ in $[0, T]$, where $t_1 = 0, t_L = T$ and

$t_l < t_{l+1}$, we model W_m^{-1} for $m = 1, \dots, M$ as

$$W_m^{-1}(t) = a_l^m t + b_l^m, \quad \text{if } t \in [t_l, t_{l+1}). \quad (8)$$

Denoting $\mathbf{a}^m = \{a_l^m\}_{l=1}^{L-1}$ and $\mathbf{b}^m = \{b_l^m\}_{l=1}^{L-1}$ as the parameters of the model, we rewrite the regularizer and the constraints of W_m^{-1} as

$$\begin{aligned} & \int_0^T \left| \frac{W_m^{-1}(s)}{M} + \frac{\sum_{m' \neq m} (W_{m'}^{k-1})^{-1}(s)}{M} - s \right|^2 ds \\ & \rightarrow \left\| \frac{1}{M} \mathbf{a}^m + \mathbf{a}^{\bar{m}} \right\|_2^2 + \left\| \frac{1}{M} \mathbf{b}^m + \mathbf{b}^{\bar{m}} \right\|_2^2, \end{aligned} \quad (9)$$

$$W_m(0) = 0 \rightarrow b_1^m = 0,$$

$$W_m(T) = T \rightarrow a_{L-1}^m T + b_{L-1}^m = T,$$

$$W_m'(t) > 0 \rightarrow a_l^m > 0 \text{ for } l = 1, \dots, L-1,$$

where $\|\cdot\|_2$ indicates the ℓ_2 norm of a vector, $\mathbf{a}^{\bar{m}} = \frac{\sum_{m' \neq m} \mathbf{a}^{m',k-1}}{M} - \mathbf{1}$ and $\mathbf{b}^{\bar{m}} = \frac{\sum_{m' \neq m} \mathbf{b}^{m',k-1}}{M}$. $\mathbf{a}^{m',k-1}$ and $\mathbf{b}^{m',k-1}$ are estimated in the previous iteration. To guarantee continuity of W_m^{-1} , we further impose the following constraints on \mathbf{a}^m and \mathbf{b}^m : for $l = 1, \dots, L-2$,

$$a_l^m t_{l+1} + b_l^m = a_{l+1}^m t_{l+1} + b_{l+1}^m. \quad (10)$$

Based on the piecewise linear model and the exponential-like intensity assumption, we propose a tight upper bound for the negative log-likelihood in (7):

$$\begin{aligned} & - \log \mathcal{L}(\theta^k; W_m^{-1}(S_m)) \\ & = \sum_{c=1}^C \int_0^T \lambda_c(W_m^{-1}(s)) ds - \sum_{i=1}^{I_m} \log \lambda_{c_i^m}(W_m^{-1}(t_i^m)) \\ & \leq \sum_{c=1}^C \int_0^T \lambda_c(s) dW_m(s) \\ & \quad - \sum_{i=1}^{I_m} \sum_{j=1}^{J_i} q_{ij}^m \log \frac{\lambda_{c_i^m}(W_m^{-1}(t_i^m))}{q_{ij}^m} \\ & = \sum_{l=1}^{L-1} \left[\frac{p_l^m}{a_l^m} + \sum_{\substack{t_i^m \in [t_l, t_{l+1}) \\ j=1, \dots, J_i}} q_{ij}^m \beta_j(a_l^m t_i^m + b_l^m) \right] + C \\ & = \mathcal{Q}(\mathbf{a}^m, \mathbf{b}^m). \end{aligned} \quad (11)$$

The intensity function is $\lambda_{c_i^m}(W_m^{-1}(t_i^m)) = \sum_{j=1}^{J_i} \alpha_j \exp(-\beta_j W_m^{-1}(t_j^m))$, the coefficients $p_l^m = \sum_c \int_{W_m^{-1}(t_l)}^{W_m^{-1}(t_{l+1})} \lambda_c(s) ds$, $q_{ij}^m = \frac{\alpha_j \exp(-\beta_j W_m^{-1}(t_j^m))}{\lambda_{c_i^m}(W_m^{-1}(t_i^m))}$ and the constant $C = \sum_{i,j} q_{ij} \log \frac{q_{ij}}{\alpha_j}$. The inequality is based on Jensen's inequality and the $\{p_l^m, q_{ij}^m\}$ are calculated based on the parameters estimated in the previous iteration. The detailed derivation and the implementations for Hawkes process and self-correcting process are given in Appendix 6.3 and 6.4.

Algorithm 1 Learning A Registered Point Process from Warped Observations (RPP-MLE)

Input: Warped sequence $\{S_m\}_{m=1}^M$, weight of regularizer γ , the landmark points $\{t_l\}_{l=1}^L$, and the maximum numbers of outer and inner iterations.

Output: Model's parameter θ and unwarping functions, parameters $\{\mathbf{a}^m, \mathbf{b}^m\}_{m=1}^M$.

```

1: Initialize  $\theta$  randomly. Set  $\mathbf{a}^m = \mathbf{1}$ ,  $\mathbf{b}^m = \mathbf{0}$  for  $m = 1, \dots, M$ .
2: repeat
3:   Given  $\{\mathbf{a}^m, \mathbf{b}^m\}_{m=1}^M$ , un warp data and update  $\theta$  by
      solving (6).
4:   for  $m = 1, \dots, M$  do
5:     repeat
6:       Given  $\{\mathbf{a}^m, \mathbf{b}^m, \theta\}$ , calculate  $\{p_i^m, q_{ij}^m\}$ .
7:       Update  $\mathbf{a}^m$  and  $\mathbf{b}^m$  by solving (12).
8:     until Converge or reach the maximum number
       of inner iterations
9:   until Converge or reach the maximum number of outer
       iterations

```

Considering (9, 10, 11) together, we propose the surrogate problem of (7):

$$\begin{aligned}
& \min_{\mathbf{a}^m, \mathbf{b}^m} \mathcal{Q}(\mathbf{a}^m, \mathbf{b}^m) + \gamma \left\| \frac{\mathbf{a}^m}{M} + \mathbf{a}^{\bar{m}} \right\|_2^2 + \gamma \left\| \frac{\mathbf{b}^m}{M} + \mathbf{b}^{\bar{m}} \right\|_2^2 \\
& \text{s.t. } 1) b_1^m = 0, a_{L-1}^m T + b_{L-1}^m = T, \\
& \quad 2) \text{for } l = 1, \dots, L-1, a_l^m > 0, \text{ and} \\
& \quad 3) a_l^m t_{l+1} + b_l^m = a_{l+1}^m t_{l+1} + b_{l+1}^m.
\end{aligned} \tag{12}$$

(12) is a typical constrained nonlinear programming problem. Many optimization methods can be applied here, *e.g.*, sequential quadratic programming and an interior-point method. Note that after getting optimal \mathbf{a}^m and \mathbf{b}^m , we need to re-calculate the $\{p_i^m, q_{ij}^m\}$ in \mathcal{Q} and solve (12) iteratively until the objective function converges.

3.4 Proposed scheme of algorithm

Repeating the two steps in the previous two subsections, we estimate the model and the warping/unwarping functions effectively. We denote our method as RPP-MLE and summarize its scheme in Algorithm 1.

Complexity Consider a C -dimensional Hawkes process as an example. We implement the MLE step and the updating of unwarping functions via an EM-based framework [40] and an interior-point method [23], respectively. Given M sequences with N events in each, the computational complexity of our method per iteration in the worst case is $\mathcal{O}(MN^2 + C^2 + ML^3)$. The $\mathcal{O}(MN^2)$ and $\mathcal{O}(C^2)$ correspond to the computational complexity of the E-step and the M-step, respectively, and the $\mathcal{O}(ML^3)$ corresponds to the computational complexity of solving M nonlinear programming with $2L$ variables per each in the worst case. Be-

cause we update unwarping functions by solving M independent optimization problems, lines 4 - 8 in Algorithm 1 can be implemented in parallel. Therefore, the time complexity of our method can be $\mathcal{O}(MN^2 + C^2 + L^3)$.

Convergence Our learning method converges in each step. For parametric point processes like Hawkes processes, their likelihood functions are convex and the convergence of the MLE-step is guaranteed. Further, the objective function in (12) is convex, as shown in Appendix 6.5, thus updating of the unwarping functions also converges well.

3.5 Justifiability Analysis

The reasons for applying piecewise linear models to warping functions are twofold. First, our learning method involves the computation of unwarping function W_m^{-1} and the derivative of warping function W_m' . Applying our piecewise linear model, both warping and unwarping functions can be represented explicitly, which simplifies the computation. If we use other basis functions, *e.g.*, Gaussian basis, to represent W_m (or W_m^{-1}), the W_m^{-1} (or W_m') will be hard to be represented in closed-form. Second, compared to the finite element analysis method used in functional optimization and differential equations, which discretizes functions into many grids, our piecewise linear model requires much fewer parameters, which reduces the risk of over-fitting and the computational complexity.

Compared with existing point process registration methods, *e.g.*, the Wasserstein learning-based registration method (WLR) [5, 22, 38] and the multi-task learning-based method (MTL) [17], our RPP-MLE method has several advantages. First, both the WLR and the MTL require learning a specific model for each event sequence. For complicated multi-dimensional point processes, they require a large amount of events per sequence to learn reliable models independently, which might be unavailable in practice. Our method has much fewer parameters, and thus has much lower computational complexity and lower risk of overfitting. Second, both the WLR and the MTL decompose the learning of model and warping functions into two independent steps. The estimation error caused in the previous step will propagate to the following one. On the contrary, our method optimizes model and warping functions alternatively and its convergence in each step is guaranteed, so the estimation error will be suppressed iteratively. Finally, the WLR is designed for learning non-parametric point processes, while our method aims to learn parametric point processes. The models we learned can be more interpretable and predictive.

4 Experiments

To demonstrate the feasibility and effectiveness of the proposed method, we compare it to existing point pro-

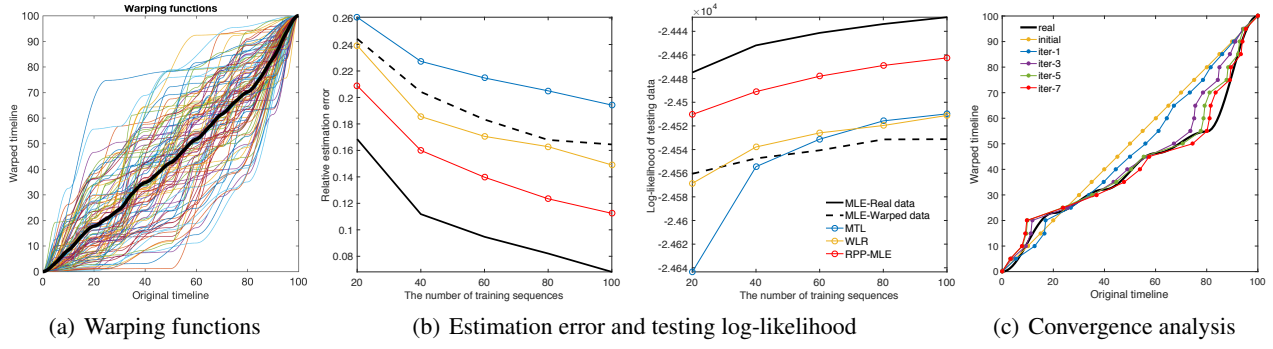


Figure 2: Experimental results of various methods on synthetic data.

cess learning and registration methods on both synthetic and real-world datasets. In particular, we compare to the following methods: purely maximum likelihood estimation based on warped observations (MLE); the multi-task learning-based method (MTL) [17]; and the Wasserstein learning-based registration method (WLR) [22]. The MTL method learns a specific parametric point process for each event sequence, and averages the learned parameters over all event sequences in the Euclidean space. The models are learned jointly in the framework of multi-task learning – the parameters corresponding to different event sequences have a low-rank and sparse structure. To the best of our knowledge, the WLR is the state-of-the-art model registration method focusing on point processes and their warped event sequences, proven to outperform many baselines like FRM [29] and PACE [30] mentioned in Section 2.2. To apply the WLR method to learn parametric point process models, we first follow the work in [22], learning the densities of observed events by kernel density estimation (KDE) [26], and learning the warping functions by finding the optimal transport between the densities and their barycenter in the Wasserstein space. Finally, we apply the reversed warping functions to un warp the observations and learn a parametric point process.

4.1 Synthetic data

We simulate 200 event sequences in the time window $[0, 100]$ based on a 4-dimensional Hawkes process using Ogata’s thinning method [21], and divide them equally into a training set and a testing set. Each sequence in the training set is modified by a specific warping function. The warping functions are visualized in Fig. 2(a), in which each color curve represents a warping function and the black bold curve represents the average of all the functions. The warping functions obey the two assumptions we imposed before, *i.e.*, each warping function is monotone increasing and the average is close to an identity function. The detailed generation process is given in Appendix 6.6.

Given the training data, we can learn registered point process models by different methods and evaluate their perfor-

mance on 1) the relative estimation error $\frac{\|\theta^* - \theta\|_2}{\|\theta\|_2}$, where θ is the ground truth and θ^* is the estimation result; and 2) the log-likelihood of testing set. For each method, we test it in 5 trials and visualize its averaged result in Fig. 2(b). The black bold curves correspond to the MLE based on unwarped data, which achieves the best performance (*i.e.*, the lowest estimation error and the highest log-likelihood), while the black dot curves correspond to the MLE based on warped data. The performance of a good registration method should be much better than the black dot curves and approach to the black bold curves. In Fig. 2(b) we can find that our RPP-MLE method achieves superior performance to MTL and WLR. The performance of MTL is even worse than that of applying MLE to warped data directly, especially in the case with few training data. This result implies that 1) the sparse and low-rank structure imposed in the multi-task learning phase cannot reflect the actual influence of warped data on the distribution of parameters; and 2) the average of the parameters in the Euclidean space does not converge well to the ground truth. The performance of WLR is comparable to that of applying MLE to warped data directly, which verifies our claim that the WLR is just suitable for the simple nonparametric cases of point processes.

Both MTL and WLR reply on a strategy of learning a specific model for each event sequence in a parametric or non-parametric way, and then averaging the models in a pre-defined space. As aforementioned, this strategy does not work when the target point process is complicated, *e.g.*, the 4-dimensional Hawkes process used in our experiment, because it ignores a fact that the number of events in a single event sequence is often insufficient to learn a reliable model in practice. Our RPP-MLE method, by contrast, learns a single registered model and all warping functions jointly in an iterative manner. Learning of the registered model and the warping functions are alternative rather than independent steps, each having a positive influence on the other. As a result, our method suppresses the risk of over-fitting and achieves much better results.

Furthermore, we illustrate the learning process of a warp-

ing function in Fig. 2(c). The black bold curve corresponds to the ground truth and the yellow line is the initialization of our estimation. We find that applying our RPP-MLE method, the learning result converges after 7 iterations and the final estimation of the warping function (the red curve) approaches the ground truth. This underscores that our method converges quickly, and the learned warping function can approximate the real idiosyncratic effect.

4.2 Real-world data

We test our method and compare it with the WLR on two real-world datasets: the MIMIC III dataset [14] and the LinkedIn dataset [34]. The MIMIC III dataset contains over ten thousand patient admission records over ten years. Each admission record is a sequence, with admission time stamps and the ICD-9 codes of diseases. Following [34], we assume that there are triggering patterns between different diseases, which can be modeled by a Hawkes process. We focus on modeling the triggering patterns between the diseases of the circulatory system, which are grouped into 8 categories. We extract 1,129 admission records related to the 8 categories as the training set. Each record can be viewed as an event sequence warped from a “standard” record because of the idiosyncratic nature of different patients. For the LinkedIn dataset, we extract 709 users having working experience in 7 IT companies. Similarly, the timeline of different users can be different, because they have different working experience and personal conditions, and the status of the job market when they jump is different as well. We want to learn a “standard” Hawkes process to measure the relationships among the companies and exclude these uncertain factors.

We apply different model registration methods to learn registered Hawkes processes from the two real-world datasets. The evaluation is challenging because both the ground truth of the model and that of the warping functions are unknown. Fortunately, we can use learning results to evaluate the risks of under- and over-registration for different methods in an empirical way. Given unwarped event sequences estimated by different methods, we learn the parameter of model θ^* and estimate its variance $\text{var}(\theta^*)$ by parametric bootstrapping [32]. For the method with a lower risk of under-registration, its learning result should be more stable and the estimated variance should be smaller. Therefore, we can use the estimated variance as a metric for the risk of under-registration, *i.e.*, $risk_{under} = \text{var}(\theta^*)$. We define the following metric to evaluate the risk of over-registration: $risk_{over} = \frac{\int_0^T |s - \bar{W}(s)|^2 ds}{\frac{1}{M} \sum_{m=1}^M \int_0^T |W_m(s) - \bar{W}(s)|^2 ds}$, where $\bar{W}(s) = \frac{1}{M} \sum_m W_m(s)$. The numerator is the distance between the mean of warping functions and an identity function, and the denominator is the variance of warping functions. When the estimated warping functions have a small variance (*i.e.*, the warping functions are similar to

Table 1: Comparison for various methods.

Data	Method	$risk_{under}$	$risk_{over}$	Rank Corr.
MIMIC-III	WLR [22]	0.018	0.055	0.025
	RPP-MLE	0.011	0.009	0.053
LinkedIn	WLR [22]	0.029	0.657	0.344
	RPP-MLE	0.025	0.010	0.375

each other) but are distinct from identity function (*i.e.*, the unbiasedness assumption is not met), it means that the corresponding method causes over-registration.

The side information of the dataset is also helpful to evaluate the appropriateness of the learning result. In Fig. 3(a), most of the admission records in the MIMIC III dataset are from relatively old patients. The incidence of circulatory system diseases is mainly correlated with patient age. Learning a “standard” patient model from a dataset dominated by old patients, we can imagine that the admission record of an old patient should be more similar to that of the “standard” patient, and the corresponding warping function should be closer to the identity function. Therefore, given the deviations between learned warping functions and the identity function, we can calculate the Kendall’s rank correlation between the warping deviations and the ages of the patients. Similarly, in Fig. 3(b), most of samples in the LinkedIn dataset are from young users with 4 or fewer working years, so these young users’ behaviors should likely be close to that of the “standard” job-hopping model learned from the data, and the warping deviations should be correlated with the working years.

Table 1 shows the comparison between our RPP-MLE method and the WLR method on these two datasets. We find that the proposed method outperforms WLR consistently on different metrics and different datasets, obtaining lower risks of under- and over-registration and higher rank correlation. In particular, the low risk of under-registration means that the parameter θ^* learned by our method is stable. The low risk of over-registration means that the warping functions we learned have good diversity while obeying the unbiasedness assumption. The high rank correlation verifies the justifiability of our method – the warping deviations of dominant samples (*i.e.*, the old patients in MIMIC III and young employees in LinkedIn data) are smaller than those of minor samples (*i.e.*, the young patients and the old employees).

Figures 3(c) and 3(d) compare the infectivity matrices¹ of the registered Hawkes processes and the warping functions learned by WLR and our RPP-MLE for the two datasets. These results further verify the superiority of our method. First, the warping functions we learned have good diversity while obeying the unbiasedness assumption better than

¹Infectivity matrix is denoted as $\Psi = [\psi_{cc'}]$. Its element is the integral of impact function over time, *i.e.*, $\psi_{cc'} = \int_0^T \phi_{cc'}(s) ds$.

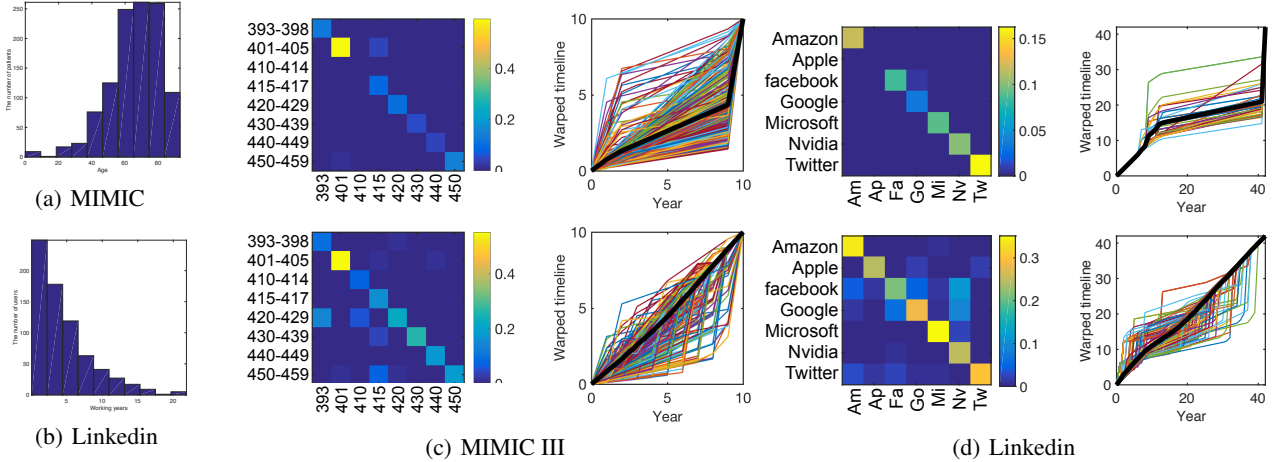


Figure 3: Experimental results of our method on real-world datasets. In (c) and (d), the first row corresponds to the infectivity matrix and the warping functions learned by WLR, and the second row corresponds to those learned by our RPP-MLE. The black bold curves are the average of warping functions.

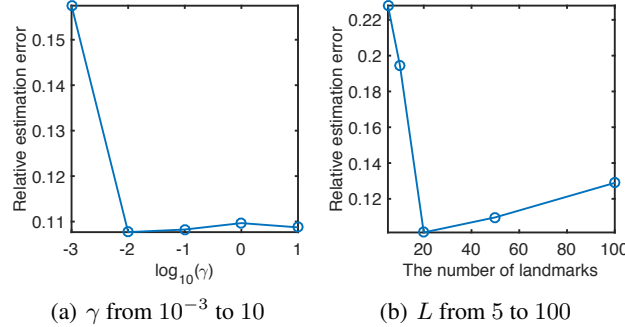


Figure 4: Illustration of robustness.

those learned by WLR. Second, the infectivity matrices learned by our RPP-MLE are more dense and informative, which reflect some reasonable phenomena that are not found by WLR. For the MIMIC III data, the infectivity matrix of WLR only reflects the self-triggering patterns of the disease categories, while ours is more informative: the 5-th row of our matrix (the bottom-left subfigure in Fig. 3(c)) corresponds to the category “other forms of heart disease” (ICD-9 code 420-429), which contains many miscellaneous heart diseases and has complicated relationships with other categories. Our learning result reflects this fact – the 5-th row of our infectivity matrix contains many non-zero elements. For the LinkedIn data, the infectivity matrix of our method reveals more information besides the self-triggering patterns: 1) The values of “Facebook-Google” and “Google-Facebook” imply that job-hopping behaviors happen frequently between Facebook and Google, which reflects fierce competition between these companies. 2) The values of “Facebook-Nvidia” and “Google-Nvidia” reflect the fact that recent years many Nvidia’s employees jump to Google and Facebook to develop the hardware of AI. More detailed analysis are given in Appendix 6.7.

4.3 Robustness analysis

We investigate the robustness of our method to variations in its parameters, including the weight of regularizer γ and the number of landmarks L . In particular, we learn models from the synthetic data by our method with different configurations, and visualize the estimation errors with respect to these two parameters in Fig. 4. The weight γ controls the importance of the regularizer, which is correlated with the strictness of the unbiasedness assumption. The larger γ , the more similarity we have between warping function and identity function. In Fig. 4(a) we find that our method is robust to the change of γ in a wide range (*i.e.*, from 10^{-3} to 1). When γ is too small (*i.e.*, $\gamma = 10^{-3}$), however, the estimation error increases because the regularizer is too weak to prevent over-registration. The number of landmarks L has an effect on the representation power of our method. In Fig. 4(b), we find that the lowest estimation error is achieved when the number of landmarks $L = 20$. When L is too small, our piecewise linear model is over-simplified and cannot fit complicated warping functions well. When L is too large, (12) has too many variables and the updating of warping function suffers to the problem of over-fitting.

5 Conclusions and Future work

We have proposed an alternating optimization method to learn parametric point processes from warped (idiosyncratic) observations. We demonstrate its justifiability and advantages relative to existing methods. Our method has potentials to many applications. For admission behavior, learning a model that captures shared and patient-specific characteristics of a disease helps evaluate the status of the patients and improve their treatments. For job-hopping behavior, learning a “standard” job-hopping process excluding the factors from employees can reflect the essential

competitions among different companies and their actual attractiveness to talents. In the future, we plan to extend our method to more complicated point process models and apply it to more applications.

6 Appendix

6.1 Exponential-like intensity functions

We give some typical and important point processes with exponential-like intensity functions. For the convenience of expression, we only consider 1-D point processes, *i.e.*, the number of event types $C = 1$, but these examples can be easily extended to multi-dimensional cases.

Hawkes processes. The intensity function of a 1-D Hawkes process is

$$\lambda(t) = \mu + \sum_{t_i < t} \phi(t - t_i), \quad (13)$$

A typical implementation of the impact function $\phi(t)$ is exponential function, *i.e.*, $\rho \exp(-wt)$ in [10, 15, 40, 37]. Therefore, we can rewrite (13) as

$$\begin{aligned} \lambda(t) &= \mu + \sum_{t_i < t} \phi(t - t_i) \\ &= \mu \exp(0t) + \sum_{t_i < t} \rho \exp(wt_i) \exp(-wt) \\ &= \sum_{j=1}^J \alpha_j \exp(-\beta_j t), \end{aligned} \quad (14)$$

where $J = 1 + |\{t_i : t_i < t\}|$. We can find that for $j = 1$, $\beta_j = 0$ and $\alpha_j = \mu$; for $j = 2, \dots, J$, $\beta_j = w$ and $\alpha_j = \rho \exp(wt_i)$.

Self-correcting processes. The intensity function of a 1-D self-correcting process [12, 36] is

$$\lambda(t) = \exp(\mu t - \sum_{t_i < t} \phi(t_i)). \quad (15)$$

Generally, $\phi(t)$ can be 1) a linear function of time, *i.e.*, $\phi(t) = \rho t$; or 2) a constant, *i.e.*, $\phi(t) = \rho$. In this case, we can simply represent $\lambda(t)$ as an exponential function $\alpha \exp(-\beta t)$, where $\alpha = \exp(-\sum_{t_i < t} \phi(t_i))$ and $\beta = -\mu$.

6.2 The proof of Theorem 3.1

Proof. Denote an original (unwarped) event sequence as D . The negative log-likelihood function of the target point process N_θ can be written as

$$-\log \mathcal{L}(\theta; D) = \int_0^T \lambda(s) ds - \sum_i \log \lambda(t_i), \quad (16)$$

where t_i is the i -th event of the sequence D . When the training sequence D is warped by a warping function

$W : [0, T] \mapsto [0, T]$ satisfying the assumptions 1 and 2, we have

$$\begin{aligned} &-\log \mathcal{L}(\theta; S) \\ &= \int_0^T \lambda(W(s)) ds - \sum_i \log \lambda(W(t_i)) \\ &= \int_0^T \lambda(s) dW^{-1}(s) - \sum_i \log \lambda(W(t_i)), \end{aligned} \quad (17)$$

where S is the warped data.

Sufficiency. When the target point process is a homogeneous Poisson process, *i.e.*, $\lambda(t) = \mu$, we can find that

$$-\log \mathcal{L}(\theta; S) = -\log \mathcal{L}(\theta; D) = T\mu - I \log \mu, \quad (18)$$

where I is the number of events. Therefore, both $\hat{\theta}^*$ and $\hat{\theta}$ are equal to $\frac{I}{T}$.

When we relax the range of $W(t)$ but assume that it is a translation, *i.e.*, $W(t) = t + \tau$, the relative distance between arbitrary two events, *i.e.*, $t_i - t_j = W(t_i) - W(t_j)$, is unchanged. Based on the stationarity of the target point process, the learning result is unchanged as well.

Necessity. When the target point process has exponential-like intensity function, the negative log-likelihood is a convex function of θ . The warping function satisfying the assumption 1 and 2 does not change the convexity of the negative log-likelihood. Therefore, when $\hat{\theta}^* = \hat{\theta}$, we have

$$\frac{\partial -\log \mathcal{L}(\theta; S)}{\partial \theta} \Big|_{\hat{\theta}^*} = 0, \quad (19)$$

for the target point process.

Even in the simplest case, *i.e.*, the intensity is a single exponential function $\lambda(t) = \alpha_\theta \exp(-\beta t)$ and only α_θ is a single coefficient related to the parameter θ , we have

$$\begin{aligned} &-\log \mathcal{L}(\theta; S) \\ &= -\log \mathcal{L}(\theta; D) + \int_0^T (1 - (W^{-1})'(s)) \lambda(s) ds \\ &\quad - \sum_i \log \frac{\lambda(W(t_i))}{\lambda(t_i)} \\ &= -\log \mathcal{L}(\theta; D) + \alpha_\theta \int_0^T (1 - (W^{-1})'(s)) \exp(-\beta s) ds \\ &\quad - \sum_i \log \frac{\exp(-\beta W(t_i))}{\exp(-\beta t_i)}. \end{aligned}$$

Here, we have

$$\frac{\partial -\log \mathcal{L}(\theta; D)}{\partial \theta} \Big|_{\hat{\theta}^*} = 0, \quad (20)$$

and the last term $-\sum_i \log \frac{\exp(-\beta W(t_i))}{\exp(-\beta t_i)}$ is a constant with respect to θ , therefore, $\frac{\partial -\log \mathcal{L}(\theta; S)}{\partial \theta} \Big|_{\hat{\theta}^*} = 0$ is equivalent to

$\int_0^T (1 - (W^{-1})'(s)) \exp(-\beta s) ds \equiv 0$ for all kinds of event sequences. This condition satisfies in two situations: 1) $(W^{-1})'(s) \equiv 1$, which corresponds to a translation function; 2) $\beta = 0$, such that $\lambda(t) = \alpha_\theta$ is a constant, which corresponds to a homogeneous Poisson process. \square

6.3 The derivation of (11)

Based on the assumption 3 of the target point process, the negative log-likelihood in (7) can be rewrite as

$$\begin{aligned}
 & -\log \mathcal{L}(\theta^k; W_m^{-1}(S_m)) \\
 &= \sum_{c=1}^C \int_0^T \lambda_c(W_m^{-1}(s)) ds - \sum_{i=1}^{I_m} \log \lambda_{c_i^m}(W_m^{-1}(t_i^m)) \\
 &= \sum_{c=1}^C \int_{W_m^{-1}(0)}^{W_m^{-1}(T)} \lambda_c(s) dW_m(s) \\
 &\quad - \sum_{i=1}^{I_m} \log \left(\sum_{j=1}^{J_i} \alpha_j \exp(-\beta_j W_m^{-1}(t_i^m)) \right) \quad (21) \\
 &= \sum_{c=1}^C \int_0^T \lambda_c(s) dW_m(s) \\
 &\quad - \sum_{i=1}^{I_m} \log \left(\sum_{j=1}^{J_i} \alpha_j \exp(-\beta_j W_m^{-1}(t_i^m)) \right) \\
 &= \mathcal{A} + \mathcal{B}.
 \end{aligned}$$

On one hand, based on the piecewise linear model of W_m^{-1} , the term \mathcal{A} can be further rewritten as

$$\begin{aligned}
 \mathcal{A} &= \sum_{c=1}^C \int_{W_m^{-1}(0)}^{W_m^{-1}(T)} \lambda_c(s) dW_m(s) \\
 &= \sum_{c=1}^C \sum_{l=1}^{L-1} \int_{W_m^{-1}(t_l)}^{W_m^{-1}(t_{l+1})} \lambda_c(s) \frac{dW_m(s)}{ds} ds \quad (22) \\
 &= \sum_{l=1}^{L-1} \underbrace{\frac{1}{a_l^m}}_{W_m'} \underbrace{\sum_{c=1}^C \int_{W_m^{-1}(t_l)}^{W_m^{-1}(t_{l+1})} \lambda_c(s) ds}_{p_l^m}.
 \end{aligned}$$

On the other hand, given current estimated parameters, we can calculate

$$\begin{aligned}
 q_{ij}^m &= \frac{\alpha_j \exp(-\beta_j W_m^{-1}(t_j^m))}{\sum_{j'} \alpha_{j'}^{J_i} \exp(-\beta_{j'} W_m^{-1}(t_{j'}^m))} \quad (23) \\
 &= \frac{\alpha_j \exp(-\beta_j W_m^{-1}(t_j^m))}{\lambda_{c_i^m}(W_m^{-1}(t_i^m))},
 \end{aligned}$$

and then apply Jensen's inequality to the term \mathcal{B} :

$$\begin{aligned}
 \mathcal{B} &= - \sum_{i=1}^{I_m} \log \left(\sum_{j=1}^{J_i} \alpha_j \exp(-\beta_j W_m^{-1}(t_i^m)) \right) \\
 &\leq \sum_{i=1}^{I_m} \sum_{j=1}^{J_i} q_{ij}^m \log \frac{q_{ij}^m}{\alpha_j \exp(-\beta_j W_m^{-1}(t_i^m))} \\
 &= \sum_{i=1}^{I_m} \sum_{j=1}^{J_i} q_{ij}^m \left(\log \frac{q_{ij}^m}{\alpha_j} + \beta_j W_m^{-1}(t_i^m) \right) \\
 &= \sum_{l=1}^{L-1} \sum_{t_i^m \in [t_l, t_{l+1})} \sum_{j=1}^{J_i} q_{ij}^m \beta_j (a_l^m t_i^m + b_l^m)) + C
 \end{aligned} \quad (24)$$

6.4 Practical implementations

Taking a **multi-dimensional Hawkes process** as an example, we give the implementation details of our learning method. Specifically, the intensity function of the type- c event at time t is

$$\lambda_c(t) = \mu_c + \sum_{t_i < t} \phi_{c_i c_j} \exp(-w(t - t_i)), \quad (25)$$

where the parameter set θ consists of the background intensity vector $\mu = [\mu_c]$ and the infectivity matrix $\Phi = [\phi_{cc'}]$.

Maximum likelihood. Given unwarped sequences $\{W_m^{-1}(S_m)\}_{m=1}^M$, we can maximize the likelihood of the sequences by an EM-based method [15, 40]. Specifically, the negative likelihood function and its tight upper bound can be written as

$$\begin{aligned}
 & - \sum_{m=1}^M \log \mathcal{L}(\theta; W_m^{-1}(S_m)) \\
 &= \sum_{m=1}^M \left[\sum_{c=1}^C \int_0^T \lambda_c(W_m^{-1}(s)) ds \right. \\
 &\quad \left. - \sum_{i=1}^{I_m} \log \lambda_{c_i^m}(W_m^{-1}(t_i^m)) \right] \\
 &= \sum_{m=1}^M \left[\sum_{c=1}^C \left(T \mu_c + \sum_{i=1}^{I_m} \phi_{cc_i^m} \int_0^{T-t_i^m} \exp(-w W_m^{-1}(s)) ds \right) \right. \\
 &\quad \left. - \sum_{i=1}^{I_m} \log \left(\mu_{c_i^m} + \sum_{j=1}^{i-1} \phi_{c_i^m c_j^m} \exp(-w \tau_{ij}) \right) \right] \\
 &\leq \sum_{m=1}^M \left[\sum_{c=1}^C \left(T \mu_c + \sum_{i=1}^{I_m} \phi_{cc_i^m} \int_0^{T-t_i^m} \exp(-w W_m^{-1}(s)) ds \right) \right. \\
 &\quad \left. - \sum_{i=1}^{I_m} \left(p_i \log \frac{\mu_{c_i^m}}{p_i} + \sum_{j=1}^{i-1} p_{ij} \log \frac{\phi_{c_i^m c_j^m} \exp(-w \tau_{ij})}{p_{ij}} \right) \right] \\
 &= \mathcal{L}(\theta | \hat{\theta}).
 \end{aligned}$$

Here, $\tau_{ij} = W_m^{-1}(t_i^m) - W_m^{-1}(t_j^m)$ and $\hat{\theta}$ is current esti-

mated parameters used to calculate $\{p_i, p_{ij}\}$ as

$$p_i = \frac{\hat{\mu}}{\hat{\lambda}_{c_i^m}(W_m^{-1}(t_i^m))}, \quad (26)$$

$$p_{ij} = \frac{\hat{\phi}_{c_i^m c_j^m} \exp(-w\tau_{ij})}{\hat{\lambda}_{c_i^m}(W_m^{-1}(t_i^m))}.$$

As a result, we can update θ by minimizing $\mathcal{L}(\theta|\hat{\theta})$, which has the following closed-form solution:

$$\mu_c = \frac{\sum_m \sum_{c_i^m=c} p_i}{MT}, \quad (27)$$

$$\phi_{cc'} = \frac{\sum_m \sum_{c_i^m=c} \sum_{c_j^m=c'} p_{ij}}{\sum_m \sum_{c_i^m=c'} \int_0^{T-t_i^m} \exp(-wW_m^{-1}(s))ds}.$$

According to the updated parameters, we can go back to calculate $\{p_i, p_{ij}\}$. Repeating the steps above till the objective function (*i.e.*, the negative log-likelihood) converges, we can obtain the optimum model given current $\{W_m\}_{m=1}^M$.

Learning unwarping functions. The key of this step is calculating the $\{p_l^m, q_{ij}^m\}$ mentioned in (22, 24). For p_l^m , we have

$$p_l^m = \sum_{c=1}^C \int_{W_m^{-1}(t_l)}^{W_m^{-1}(t_{l+1})} \lambda_c(s) ds$$

$$= \sum_{\substack{c=1, \dots, C \\ t_i^m \in [t_l, t_{l+1}]}} \left(\phi_{cc_i^m} \int_0^{W_m^{-1}(t_{l+1}) - W_m^{-1}(t_i^m)} e^{-ws} ds \right. \\ \left. + \mu_c (W_m^{-1}(t_{l+1}) - W_m^{-1}(t_l)) \right) \quad (28)$$

$$= \sum_{\substack{c=1, \dots, C \\ t_i^m \in [t_l, t_{l+1}]}} \left(\phi_{cc_i^m} \frac{1 - e^{-wa_l^m(t_{l+1} - t_i^m)}}{w} \right. \\ \left. + \mu_c a_l^m (t_{l+1} - t_l) \right).$$

For q_{ij}^m , because

$$\lambda_{c_i^m}(W_m^{-1}(t_i^m))$$

$$= \mu_{c_i^m} + \sum_{j=1}^{i-1} \phi_{c_i^m c_j^m} \exp(-w(W_m^{-1}(t_i^m) - W_m^{-1}(t_j^m))) \quad (29)$$

$$= \sum_{j=0}^{i-1} \alpha_j \exp(-\beta_j W_m^{-1}(t_i^m)),$$

where for $j = 0$, $\alpha_j = \mu_{c_i^m}$ and $\beta_j = 0$; and for $j > 0$, $\alpha_j = \phi_{c_i^m c_j^m} \exp(wW_m^{-1}(t_j^m))$ and $\beta_j = w$, we have

$$q_{ij}^m = \frac{\alpha_j \exp(-\beta_j W_m^{-1}(t_i^m))}{\lambda_{c_i^m}(W_m^{-1}(t_i^m))} \text{ for } j = 0, \dots, i-1. \quad (30)$$

In our experiments, we configure our learning algorithm as follows. The number of landmarks $L = 20$. The weight

of regularizer $\gamma = 0.01$. The maximum number of outer iteration is 7. The maximum number of inner iteration for learning the Hawkes process model is 15. The maximum number of inner iteration for updating warping functions is 5. The interior-point method is applied.

6.5 The convexity of (12)

Ignoring constraints, (12) can be decomposed into $2(L-1)$ problems with respect to each a_l^m and b_l^m . The objective function in (12) that is related to a_l^m can be formulated as

$$f(x) = \frac{\alpha}{x} + \beta x + (x + \tau)^2, \quad (31)$$

where the unknown variable $x > 0$, the coefficients α and β are nonnegative, and τ is arbitrary. Because when $x > 0$, $\frac{\alpha}{x}$, βx and $(x + \tau)^2$ are convex functions, their sum, *i.e.*, $f(x)$, is also a convex function as well. Similarly, the objective function in (12) that is related to b_l^m can be formulated as

$$f(x) = \beta x + (x + \tau)^2, \quad (32)$$

which is also a convex function.

6.6 Generating warping functions

For the synthetic data used in our experiments, each warping function in $[0, T]$ is represented by a set of local cosine basis as

$$W_m(t) = \sum_{n=1}^N w_n^m f_n(t),$$

$$f_n(t) = \begin{cases} \cos^2(\frac{\pi}{2\Delta}(t - t_n)), & |t - t_n| \leq \Delta \\ 0, & \text{otherwise.} \end{cases} \quad (33)$$

The time window $[0, T]$ is segmented by N landmarks $\{t_n\}_{n=1}^N$, where $t_1 = 0$ and $t_N = T$. For each $f_n(t)$, the landmark t_n is its center and Δ is the distance between adjacent landmarks. The first $N-1$ coefficients $\{w_n^m\}_{n=1}^{N-1}$ is sampled from $[0, T]$ uniformly and sorted by ascending order. The last coefficient w_N^m is set to be T . Using this method, we can ensure that all warping functions are monotone increasing maps from $[0, T]$ to $[0, T]$ and their average is close to an identity function.

6.7 Details of experiments

The categories of the diseases of circulatory system are shown below:

1. Chronic rheumatic heart disease (ICD-9: 393 - 398)
2. Hypertensive disease (ICD-9: 401 - 405)
3. Ischemic heart disease (ICD-9: 410 - 414)
4. Diseases of pulmonary circulation (ICD-9: 415 - 417)

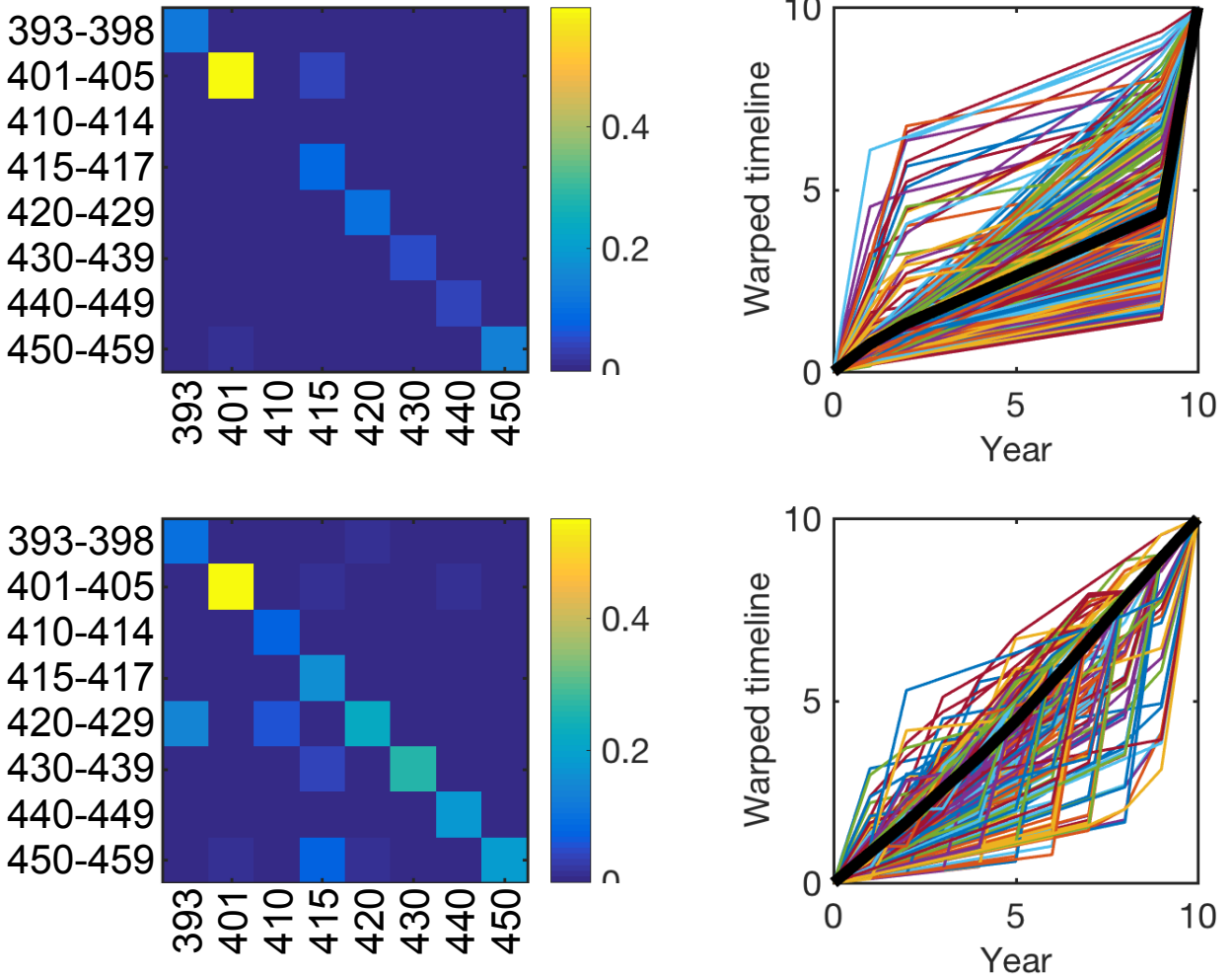


Figure 5: Experimental result of WLR (top) and our method (bottom) on MIMIC III data.

5. Other forms of heart disease (ICD-9: 420 - 429)
6. Cerebrovascular disease (ICD-9: 430 - 438)
7. Diseases of arteries, arterioles, and capillaries (ICD-9: 440 - 449)
8. Diseases of veins and lymphatics, and other diseases of circulatory system (451 - 459)

Using our RPP-MLE method, we learn a 8-dimensional Hawkes process from 1,129 patient's admission records. Compared to synthetic data, the MIMIC III dataset is sparse (*i.e.*, most of the patients have just 2 - 5 admission events), so we use a larger weight for regularizer (*i.e.*, $\gamma = 10$) and fewer landmarks (*i.e.*, $L = 5$). Similarly, we can learn a 7-dimensional Hawkes process from 709 users' job hopping records, in which we also set $\gamma = 10$ and $L = 5$.

These infectivity matrices further verify the justifiability of our learning method because they reflect some reasonable phenomena. In Fig. 5, we can find that:

1. All disease categories have strong self-triggering patterns. The "hypertension disease" (ICD-9 code 404-405), which is one of the most common disease in modern society, has the strongest self-triggering pattern — the value of the second diagonal element is over 0.5. It means that for a patient suffering to a certain disease of circulatory system, he or she is likely to re-admit to hospital in next 10 years for the same disease.
2. The 5-th row in Fig. 5 corresponds to the category "other forms of heart disease" (ICD-9 code 420-429). According to its name we can know that this category contains many miscellaneous heart diseases and should have complicated relationships with other categories. Our learning result reflects this fact — the 5-th row of our infectivity matrix contains many non-zero elements, which means that this disease category can be triggered by other disease categories.

In Fig. 6, we can find that:

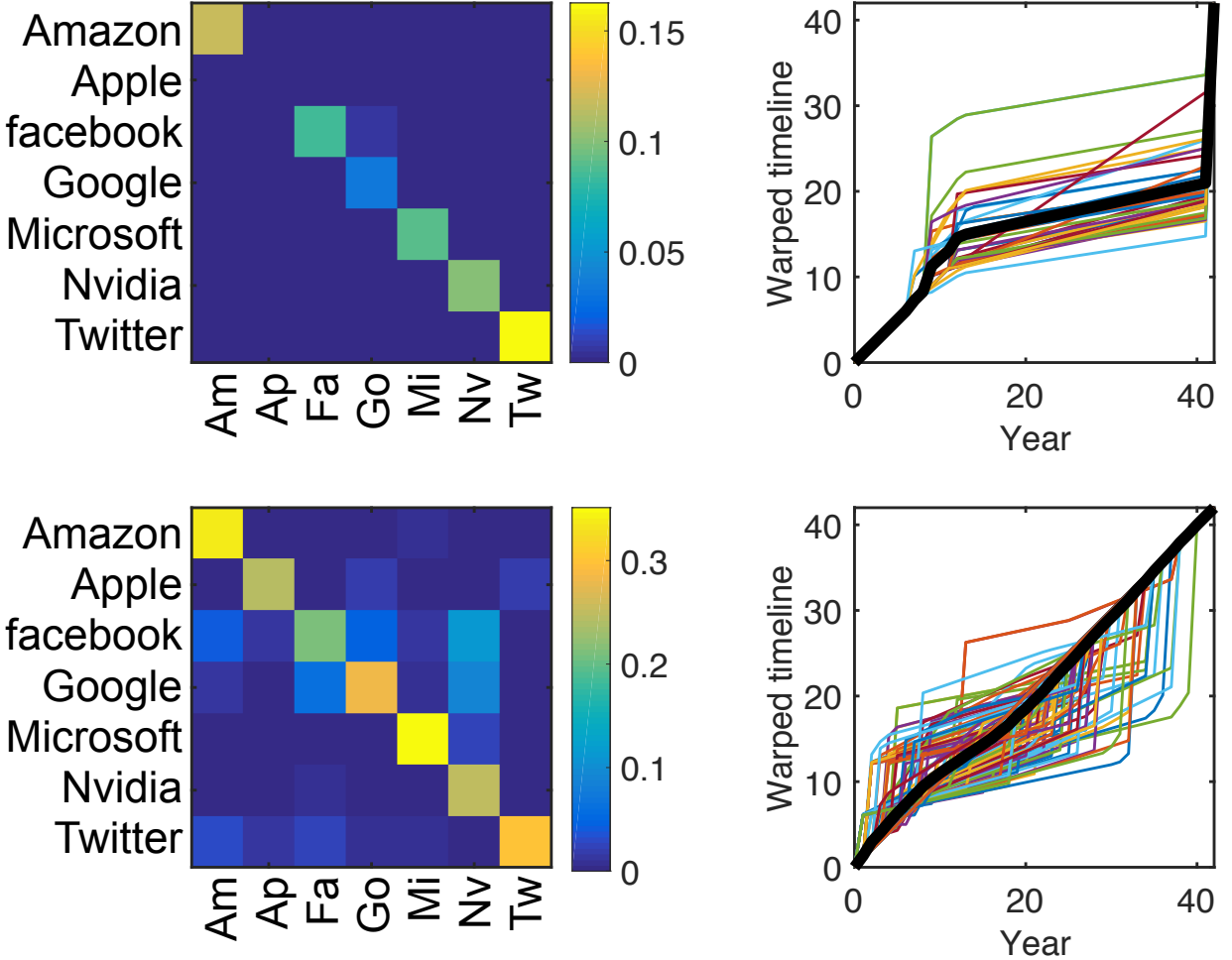


Figure 6: Experimental result of WLR (top) and our method (bottom) on LinkedIn data.

1. All IT companies have strong self-triggering patterns, which means that most of employees are satisfied to their companies. Especially for Amazon and Microsoft, their diagonal elements are over 0.3. It means that the expected happening rate of internal promotion for their employees is about 0.3 event per year.
2. The elements of “Facebook-Google” and “Google-Facebook” pairs are with high values, which means that job hopping happens frequently between Facebook and Google. This result reflects their fierce competition.
3. The elements of “Facebook-Nvidia” and “Google-Nvidia” are with high values, which reflects the fact that recent years many Nvidia’s employees jump to Google and Facebook to develop hardware and systems of AI.

References

- [1] E. Anderes, S. Borgwardt, and J. Miller. Discrete Wasserstein barycenters: optimal transport for discrete data. *Mathematical Methods of Operations Research*, 84(2):389–409, 2016.
- [2] M. Arjovsky, S. Chintala, and L. Bottou. Wasserstein GAN. *arXiv preprint arXiv:1701.07875*, 2017.
- [3] E. Bacry, K. Dayri, and J.-F. Muzy. Non-parametric kernel estimation for symmetric Hawkes processes. application to high frequency financial data. *The European Physical Journal B*, 85(5):1–12, 2012.
- [4] D. J. Berndt and J. Clifford. Using dynamic time warping to find patterns in time series. In *KDD workshop*, 1994.
- [5] J. Bigot, T. Klein, et al. Consistent estimation of a population barycenter in the Wasserstein space. *ArXiv e-prints*, 2012.
- [6] J. Cunningham, Z. Ghahramani, and C. E. Rasmussen. Gaussian processes for time-marked time-series data. In *AISTATS*, 2012.
- [7] M. Cuturi and M. Blondel. Soft-dtw: a differentiable loss function for time-series. *arXiv preprint arXiv:1703.01541*, 2017.

[8] D. J. Daley and D. Vere-Jones. *An introduction to the theory of point processes: volume II: general theory and structure*, volume 2. Springer Science & Business Media, 2007.

[9] D. Gervini and T. Gasser. Self-modelling warping functions. *Journal of the Royal Statistical Society: Series B (Statistical Methodology)*, 66(4):959–971, 2004.

[10] A. G. Hawkes and D. Oakes. A cluster process representation of a self-exciting process. *Journal of Applied Probability*, 11(3):493–503, 1974.

[11] W. Herlands, A. Wilson, H. Nickisch, S. Flaxman, D. Neill, W. Van Panhuis, and E. Xing. Scalable gaussian processes for characterizing multidimensional change surfaces. In *AISTATS*, 2016.

[12] V. Isham and M. Westcott. A self-correcting point process. *Stochastic Processes and Their Applications*, 8(3):335–347, 1979.

[13] G. M. James. Curve alignment by moments. *The Annals of Applied Statistics*, pages 480–501, 2007.

[14] A. E. Johnson, T. J. Pollard, L. Shen, L.-w. H. Lehman, M. Feng, M. Ghassemi, B. Moody, P. Szolovits, L. A. Celi, and R. G. Mark. MIMIC-III, a freely accessible critical care database. *Scientific data*, 3, 2016.

[15] E. Lewis and G. Mohler. A nonparametric EM algorithm for multiscale Hawkes processes. *Journal of Nonparametric Statistics*, 1(1):1–20, 2011.

[16] X. Liu and H.-G. Müller. Functional convex averaging and synchronization for time-warped random curves. *Journal of the American Statistical Association*, 99(467):687–699, 2004.

[17] D. Luo, H. Xu, Y. Zhen, X. Ning, H. Zha, X. Yang, and W. Zhang. Multi-task multi-dimensional Hawkes processes for modeling event sequences. In *IJCAI*, 2015.

[18] E. Mammen. Nonparametric estimation of locally stationary hawkes processes. *arXiv preprint arXiv:1707.04469*, 2017.

[19] R. Moeckel and B. Murray. Measuring the distance between time series. *Physica D: Nonlinear Phenomena*, 102(3-4):187–194, 1997.

[20] M. Musculus and S. Verduyn-Lunel. Wasserstein distances in the analysis of time series and dynamical systems. *Physica D: Nonlinear Phenomena*, 240(1):45–58, 2011.

[21] Y. Ogata. On Lewis’ simulation method for point processes. *IEEE Transactions on Information Theory*, 27(1):23–31, 1981.

[22] V. M. Panaretos, Y. Zemel, et al. Amplitude and phase variation of point processes. *The Annals of Statistics*, 44(2):771–812, 2016.

[23] F. A. Potra and S. J. Wright. Interior-point methods. *Journal of Computational and Applied Mathematics*, 124(1):281–302, 2000.

[24] J. O. Ramsay and X. Li. Curve registration. *Journal of the Royal Statistical Society: Series B (Statistical Methodology)*, 60(2):351–363, 1998.

[25] F. Roueff, R. Von Sachs, and L. Sansonnet. Locally stationary hawkes processes. *Stochastic Processes and their Applications*, 126(6):1710–1743, 2016.

[26] S. J. Sheather and M. C. Jones. A reliable data-based bandwidth selection method for kernel density estimation. *Journal of the Royal Statistical Society. Series B (Methodological)*, pages 683–690, 1991.

[27] E. Snelson, Z. Ghahramani, and C. E. Rasmussen. Warped gaussian processes. In *NIPS*, 2004.

[28] J. Snoek, K. Swersky, R. Zemel, and R. Adams. Input warping for bayesian optimization of non-stationary functions. In *ICML*, 2014.

[29] A. Srivastava, W. Wu, S. Kurtek, E. Klassen, and J. Marron. Registration of functional data using Fisher-Rao metric. *arXiv preprint arXiv:1103.3817*, 2011.

[30] R. Tang and H.-G. Müller. Pairwise curve synchronization for functional data. *Biometrika*, 95(4):875–889, 2008.

[31] Y. Wang, D. J. Miller, K. Poskanzer, Y. Wang, L. Tian, and G. Yu. Graphical time warping for joint alignment of multiple curves. In *NIPS*, 2016.

[32] L. Wassermann. *All of nonparametric statistics*. Springer Science+ Business Media, New York, 2006.

[33] S. Xiao, M. Farajtabar, X. Ye, J. Yan, L. Song, and H. Zha. Wasserstein learning of deep generative point process models. *arXiv preprint arXiv:1705.08051*, 2017.

[34] H. Xu, D. Luo, and H. Zha. Learning Hawkes processes from short doubly-censored event sequences. In *ICML*, 2017.

[35] H. Xu, W. Wu, S. Nemati, and H. Zha. Patient flow prediction via discriminative learning of mutually-correcting processes. *IEEE transactions on Knowledge and Data Engineering*, 29(1):157–171, 2017.

[36] H. Xu, Y. Zhen, and H. Zha. Trailer generation via a point process-based visual attractiveness model. In *IJCAI*, 2015.

[37] J. Yan, C. Zhang, H. Zha, M. Gong, C. Sun, J. Huang, S. Chu, and X. Yang. On machine learning towards predictive sales pipeline analytics. In *AAAI*, 2015.

[38] Y. Zemel and V. M. Panaretos. Fréchet means and Procrustes analysis in Wasserstein space. *arXiv preprint arXiv:1701.06876*, 2017.

[39] Q. Zhao, M. A. Erdogdu, H. Y. He, A. Rajaraman, and J. Leskovec. SEISMIC: A self-exciting point process model for predicting tweet popularity. In *KDD*, 2015.

[40] K. Zhou, H. Zha, and L. Song. Learning social infectivity in sparse low-rank networks using multi-dimensional Hawkes processes. In *AISTATS*, 2013.